The comparative effect of particle size and support acidity on hydrogenation of aromatic ketones

Dr. Kyung Duk Kim[†],Dr. Zichun Wang[†], Yongwen Tao[†], Dr. Huajuan Ling[†], Yuan Yuan[‡], Dr. Cuifeng Zhou[†], Prof. Dr. Zongwen Liu[†], Prof. Dr. Marianne Gaborieau[⊥], Prof. Dr. Jun Huang[†,], and Prof. Dr. Aibing Yu[§,]**

† Laboratory for Catalysis Engineering, School of Chemical and Biomolecular Engineering, The University of Sydney, NSW 2006, Australia

‡ School of Chemistry, University of New South Wales, Sydney, NSW 2052, Australia

⊥ Molecular Medicine Research Group, School of Science and Health, Australian Centre for Research of Separation Science (ACROSS), Western Sydney University, Parramatta NSW 2150, Australia

§ Laboratory for Simulation and Modelling of Particulate Systems, Department of Chemical Engineering, Monash University, Clayton, VIC 3800, Australia

ABSTRACT A comparative study was reported for both the effects of shape-confined cubic Pd particle size (8, 13, and 21 nm) and surface property of most commonly used supports (SiO_2, Al_2O_3, and silica-alumina) on catalytic performance in the chemoselective hydrogenation of three model bio-oil chemicals (benzaldehyde, acetophenone, and butyrophenone). The results showed that the size of Pd particles could be more associated with the hydrogenation reaction than acidities of the supports. Smaller size of Pd particles, regardless of the type of the support, provided the higher catalytic performance. XPS data showed that the electronic properties of Pd particles were similar, therefore, the possible reasons were the higher fraction of Pd atoms on corner in smaller particles, the lower accessibility of hydrogen atom to reactant on bigger particles, and the more low-coordinated sites in the small-size particles due to the short-range ordering. In addition, Pd/SA catalysts (Brønsted acid sites on the support) showed the highest conversion and TOF compared to Pd/Al_2O_3 and Pd/SiO_2 catalysts. This might be due to the enhanced the diffusion rates of the chemicals on the surface of the catalysts although they could not induce the ionic effect from the metal surface. Pd/SiO_2 catalysts performed better than Pd/Al_2O_3 catalysts (Lewis acid sites on the support). The flexible SiOH groups on surface made the easy interaction with the metal particles and promote the reaction.

■ INTRODUCTION

Biomass derived ketones and aldehydes can be further upgraded by the chemoselective hydrogenation, to qualified fuels or valuable unsaturated alcohols as feedstocks for drugs and fragrance.[1, 2] The challenge is to design new catalysts for reaching the desired chemoselectivity and avoiding thermodynamically favoured by-products.[3, 4] Recently, approaches to improve the efficiency of supported metal nanocatalysts have been intensively investigated. One strategy for enhancing catalytic activity or selectivity is to control the features of metal nanoparticles.[5] The hydrogenation activity and selectivity can be strongly influenced by metal particle size and dispersion. Often, reducing the particle size can introduce more unsaturated surface sites with higher surface free energy of metal species, which can promote surface reactions, for instance, the acrolein hydrogenation activity increased with decreasing Au particle size from 8 to 4 nm on Au/ZrO_2.[6] However, the acrolein hydrogenation can be enhanced with increasing the Ag particle size on Ag/SiO_2 from 1 to 9 nm.[7] It has also been observed that hydrogenation of 2-cyclohexenone over Rh/SiO_2 is size insensitive.[8] Obviously, the particle size of metal catalysts should definitely influence their catalytic performance. Therefore, understanding the size effect of metal nanoparticles is a key to tune their catalytic performance in target hydrogenation reactions.

The performance metal nanocatalysts can strongly influence by the nature of metals and supports. Normally, the acidic supports can inhibit metal aggregation, provide a large surface to volume ratio as compared to the bulk equivalents, and enhance the electron deficiency of the active metal via metal-support interaction.[9-13] The metal-support interaction can be generated through the acidic sites withdrawing electrons from the metal surface, which results in ionic effects and tunes the surface electronic properties of metal particles.[3, 9, 14] With increase the support acidity, the XPS binding energy and Fermi level of Pd supported on zeolite LTL increases, leading to

increase the difference in energy between the Pd–H antibonding orbital, which enhance the activity of Pd catalysts in neopentane hydrogenolysis reaction.[15] Moreover, extensive works focus on the preparation of Pd particle with uniform size to control their catalytic performance.[16-18] Recently, uniform Pd particles (1-2 nm) supported on various metal oxides (SiO_2, Al_2O_3 and silica-alumina) having different acidities under control are prepared by double flame-spray pyrolysis techniques.[3, 19] In these works, the Pd particles exhibit similar surface electronic properties independent from support acidity by decoupling the interaction between metal and support. This is obviously different from the metal particle size and electron properties varies from support composition/acidity prepared by classical methods, particularly on non-porous metal oxide support.[20, 21] As the supported metal catalysts prepared via impregnation techniques, it is difficult to control the properties of the final catalysts due to the strong interaction between metal and supports. Therefore, the evaluation of the metal catalyst activity based on the particle sizes of metal nanocatalysts and the properties of the supports individually is still open, however, which is necessary to understand the effects of particle size and supports on hydrogenation reactions, such as in the hydrogenation of ketones and aldehydes.

Chemoselective hydrogenation of carbonyl compounds, such as acetophenone,[3, 14, 19, 22] benzaldehyde,[23, 24] and butyrophenone are important industrial chemical process in the production of gasoline-oil and flavours, fragrances, agrochemicals, and pharmaceuticals.[23, 25] The chemoselective hydrogenation reaction of the carbonyl groups, other than phenyl groups, is important to reduce the consumption of the expensive hydrogen. The chemoselective hydrogenations of these compounds are sensitive to the surface properties of metal particles and support acidity,[9, 10] which can be utilized to evaluate the effect of metal properties and the metal-support interaction.

In this work, uniform cubic Pd nanoparticles with different particle sizes (8, 13, and 21 nm) but the same geometrical properties were synthesized by colloidal-metal nanoparticle preparation technique and loaded on SiO_2, Al_2O_3, and silica-alumina supports. Therefore, the morphology and metal loading are performed in a control manner. XPS analysis demonstrates Pd nanoparticles showing similar electronic properties over different supports. Therefore, the effects of Pd particle size and the support acidity on the catalytic performance of the supported Pd catalysts can be investigated in the hydrogenation reaction, such as in the chemoselective hydrogenation of three bio-oil model compounds (benzaldehyde, acetophenone, and butyrophenone).

■ EXPERIMENTAL

Chemicals. All chemicals employed for material synthesis and catalytic reaction, including poly(vinyl pyrrolidone) (PVP), L-ascorbic acid, potassium bromide (KBr), sodium tetrachloropalladate (II) (Na_2PdCl_4, 99.99% pure on metals basis), acetophenone (Aph, 99%), benzaldehyde (BA, 99 %), and butyrophenone (Bph, 99 %), etc. were purchased from Sigma-Aldrich.

Preparation of Pd/SA catalysts. Size-controlled Pd nano-particles were prepared by modifying a previously reported method.[26-32] PVP (Mw = 55000, 105 mg) (colloidal stabilizer), L-ascorbic acid (60 mg) (reductant) and KBr (75 mg, 300 mg and 600 mg for Pd particle size of 8 nm, 13nm and 21 nm, respectively) (capping agent), were all dissolved in deionized water (8 ml) in a 25 ml round-bottom flask at room temperature. The mixture was heated at 80 ^oC for 3 hours under magnetic stirring, resulting in a dark brown solution. For preparing Pd particle with a size of 13 and 21 nm, an additional sodium tetrachloropalladate (II) (Na_2PdCl_4) solution (57 mg) water solution (3 ml) was added into the mixture after heating for 10 minutes. Then the mixture was

cooled down, washed 3 times with deionized water and the black products (Pd nanoparticles) were collected by centrifugation at 15000 rpm.

The support materials (SiO_2, Al_2O_3, or, Silica-alumina) were prepared according to those reported in literatures.[33, 34] Pd nanoparticles was pre-dissolved in ethanol (1 mg/ml) and sonicated for 3 h at room temperature. Then a desired amount of the solution and support (2 wt % Pd) was mixed, and stirred overnight under room temperature. Then, the mixture was sonicated for 30 min, and the product was separated by centrifugation (3000 rpm) and dried in an oven at 100 ºC overnight.

Catalyst characterizations. *BET measurements.* The Brunauer-Emmett-Teller (BET) was performed by an Autosorb IQ-C system to determine the BET specific surface areas from the adsorption data obtained at P/P_0 between 0.1 and 0.3. Before measurements, the samples were degassed at 200 °C under vacuum to remove adsorbents from the surface. The specific surface areas were determined at -200 ºC by BET measurement.

X-ray Diffraction. SIEMENS X-Ray Diffractometer (XRD-D5000) with Cu Kα radiation was operated at 40 kV and 30 mA in the scan range of 1 to 70 degrees with continuous scanning mode at a rate of 2° min^{-1} (0.1542 nm wavelength).

Transmission Electron Microcopy. TEM images were obtained by using a Jeol 2200FS (200 kV). The specimens were mounted on a carbon-coated copper grid by drying a droplet of a suspension of the ground sample in ethanol.

CO chemisorption. Pd dispersion was determined by CO-pulse chemisorption on a Micromeritics Autochem II 2920 unit. Off-gas was analysed via a mass spectrometer to derive the amount of chemisorbed CO.

X-ray photoelectron spectroscopy (XPS). The supported Pd catalysts wre analyzed by XPS (ESCALAB250Xi spectrometer, Thermo Scientific, UK), which was equipped with a mono-chromated Al K (1486. 68 eV) X-ray source and operated at 15.2 kV and 164 W (10.8 mA). The catalyst powder was measured in the vacuum chamber (2×10^{-9} mbar) and the photoelectron take-off angle was 90º with respect to the surface of the sample.

Solid state NMR spectroscopy. The ^{27}Al MAS (magic-angle spinning) NMR investigation of catalysts was carried out on a Bruker DPX 200 WB spectrometer at resonance frequency of 52 MHz with a sample spinning rate of 8 kHz using 4 mm MAS rotors. Before measurements, all the samples were exposed to a saturated vapour of a $Ca(NO_3)_2$ solution at ambient temperature overnight in a desiccator for full hydration. Power levels and chemical shift scales were calibrated with respect to aqueous aluminium nitrate (with a chemical shift of 0 ppm). Spectra were recorded after single–pulse π/6 excitations with a repetition time of 0.5s for studying ^{27}Al nuclei.

TPD characterization. Temperature programmed desorption of ammonia (NH_3-TPD) was performed on a Chem BET TPR/TPD Chemisorption Analyzer, CBT-1, manufactured by QuantaChrome instruments. Prior to TPD, the sample (30 mg) was loaded and degassed at 520 ºC for 1 h under a He flow rate of 120 ml/min to completely remove molecules adsorbed on catalyst surface. Then the sample was saturated with NH_3 at 100 ºC, and flushed with a He flow (120 ml/min), then desorbed NH_3 with increasing temperature from 50 ºC up to 1000 ºC at a rate of 10 ºC /min. The concentration of desorbed ammonia was analyzed by a TCD detector connected to the TPD system.

Chemoselective hydrogenation of bio-oil model compounds. Pd/SA catalysts were put in an autoclave which was purged three times with nitrogen. Acetophenone (30mg) was dissolved in purified water (6 ml) and then added to the autoclave. The reaction was carried out at a hydrogen

pressure of 3 bar at 65 ºC under magnetic stirring for 3 h with a Pd/Aph molar ratio of 1:62.5. The reaction product(s) were collected at intervals of 10, 20, 30, 45, 60, 90, 120 and 180 min. Chemoselective hydrogenation of BA was carried out in a similar manner, in which, BA (30 mg) replaced Aph and the reaction was performed at 25 ºC with a Pd/BA molar ratio of 1:75. For chemoselective hydrogenation of Bph, Bph (30 mg) was dissolved in 2-propanol (6 ml). Then the reaction was carried out in autoclave at 65 ºC with 3 bar hydrogen pressure with a Pd/Bph molar ratio of 1:50. The conversion and composition of the product mixtures were analyzed using a Shimadzu GCMS-QP2010 Ultra with a RTX-5MS capillary column (30 m × 0.25 mm × 0.25 μm) and quantified by Shimadzu GC-FID equipped with a RTX-5 capillary column (30 m × 0.32 mm × 3 μm). Bicyclohexyl (0.1 mmol) was used as an internal standard. The selectivity to specific product(s) i (S_i) was calculated as S_i (%) = (c_i)/[(c_{APh})$_0$-(c_{APh})], where (c_i) is the molar concentration of the products, such as 1-phenylehtanol (PhE), and (c_{APh})$_0$ and (c_{APh}) correspond to the molar concentration of acetophenone before and after the reaction, respectively. TOF was calcualted as (moles of substrate converted)/(moles of Pd center x dispersion) at specific time (s) of the conversion of about 10 % of reactant.

■ RESULTS AND DISCUSSION

Characterization of catalysts. The size and shape of as-synthesized Pd particles were studied by TEM. The synthesis is based on a water-based process that involves addition of Na_2PdCl_4 into an mixture solution of L-ascorbic acid (reductant) at 80 ºC and poly(vinyl pyrrolidone) (PVP) working as a stabilizer and Br^- ions serving as a capping agent. Control over the size of the Pd cubes was achieved by adjusting the rate of reduction of $Pd2^+$ ions with Br^- ions. As shown in Supporting Information Figure S1 and S2, the average Pd particle sizes (8, 13 and 21 nm) increased with increasing the amount of the reducing agent (KBr: 75, 300, and 600 mg), respectively, in

good consistent with previous literatures.[30-32] All Pd particles showed the same cubic morphology (Figure S1). These Pd particles can sustain their morphology even after loading on different support materials (Figure 1 and S3-4). It demonstrates the Pd particles are stable under current conditions.

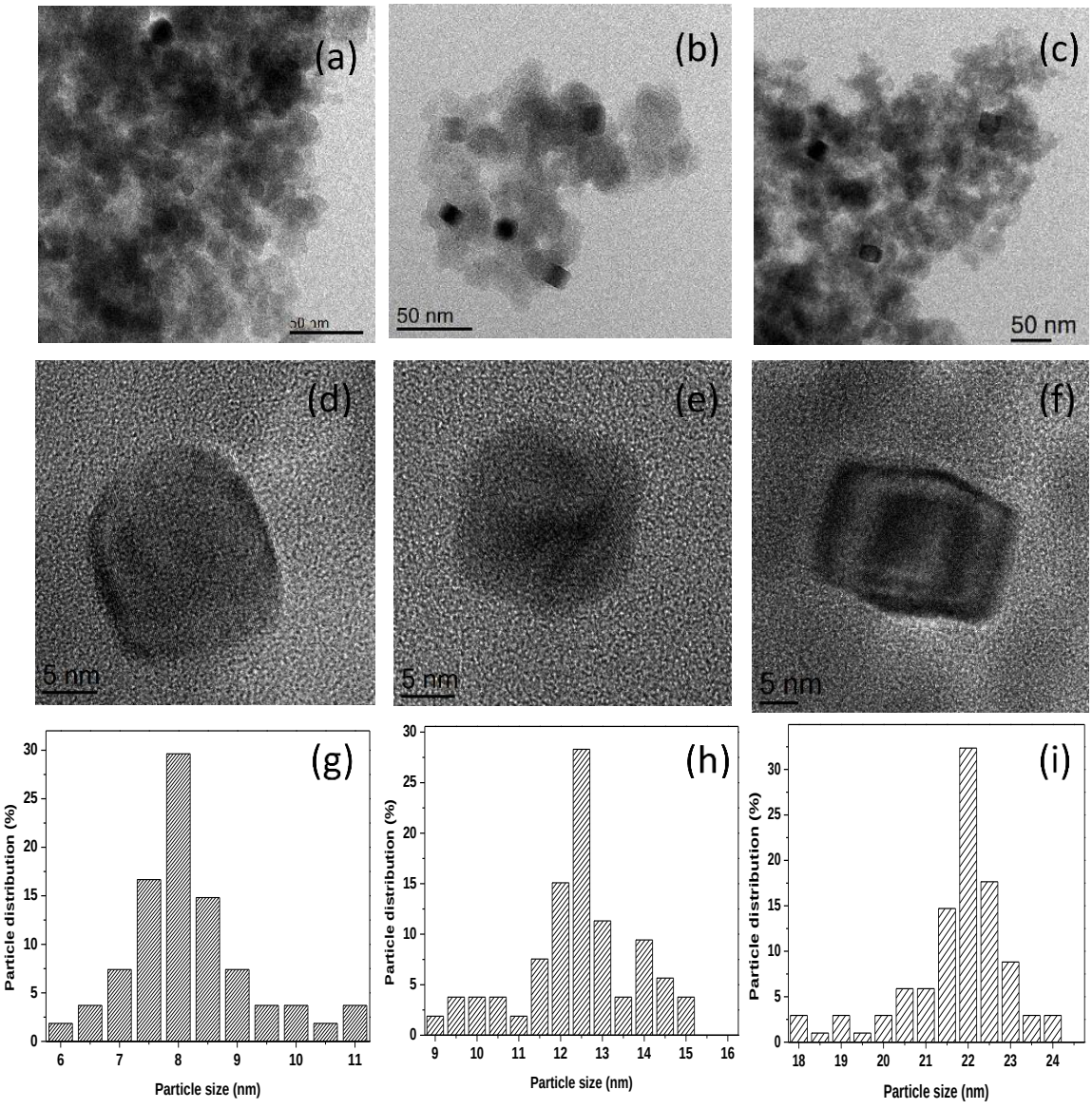

Figure 1. TEM and HRTEM images of particle distributions of silica-alumina supported samples, and Pd particle distributions: (a) TEM of Pd/SA-8, (b) TEM of Pd/SA-13, (c) TEM of Pd/SA-21 Pd particle size distribution of Pd/ SA-8, (d) HRTEM of Pd/ SA -8, (e) HRTEM of Pd/SA-13, (f)

HRTEM of Pd/SA-21 Pd particle size distribution of Pd/SA- 13, (g) TEM of Pd/SA-8, (h) Pd particle size distribution of Pd/SA- 13, and (i) Pd particle size distribution of Pd/SA- 21.

BET surface areas of Pd catalysts on different supports were determined by nitrogen adsorption-desorption isotherm and summarized in Table 1. The surface areas of Pd/SA, Pd/SiO_2 and Pd/Al_2O_3 were 171 to 167 m^2/g, 309 to 297 m^2/g, and 119 to 112 m^2/g, respectively. Compared to the parent support materials,[33, 34] Pd loading and their particle size have very slight effect on the surface area of Pd supported catalysts. The surface areas increased with increasing the content of silica, in a good agreement that silica often exhibits a larger surface areas than that of γ-Al_2O_3.[19, 35]

Table 1. Specific surface area, particle size, dispersion, and Turnover Frequencies (TOF) for the Chemoselective Hydrogenation of acetophenone, benzaldehyde, and butyrophene over Pd supported catalysts.

Sample	A_{BET} $(m^2g^{-1})^a$	P_{Pd} (nm)[b]	D_{Pd} (%)[c]	TOF_{Aph} $(s^{-1})^d$	TOF_{BA} $(s^{-1})^d$	TOF_{Bph} $(s^{-1})^d$
Pd/SA-8	171	8.0	17.1	2.2×10^{-2}	5.2×10^{-2}	2.1×10^{-2}
Pd/SA-13	168	12.6	10.5	1.6×10^{-2}	4.5×10^{-2}	1.6×10^{-2}
Pd/SA-21	167	21.6	5.5	1.0×10^{-2}	3.2×10^{-2}	0.8×10^{-2}
Pd/SiO_2-8	309	8.5	16.5	1.4×10^{-2}	4.2×10^{-2}	1.9×10^{-2}
Pd/SiO_2-13	300	13.2	12.5	1.1×10^{-2}	3.3×10^{-2}	1.7×10^{-2}
Pd/SiO_2-21	297	21.2	5.1	0.9×10^{-2}	2.9×10^{-2}	0.8×10^{-2}
Pd/Al_2O_3-8	119	8.4	16.9	1.1×10^{-2}	3.2×10^{-2}	1.2×10^{-2}
Pd/Al_2O_3-13	117	12.9	11.9	1.0×10^{-2}	2.1×10^{-2}	1.0×10^{-2}
Pd/Al_2O_3-21	112	21.8	5.9	0.7×10^{-2}	1.3×10^{-2}	0.5×10^{-2}

[a] Surface area (A_{BET}) was determined by BET analysis. [b] Pd particle size (P_{Pd})was obtained from corresponding TEM images. [c] Pd dispersion (D_{Pd}) was determined by CO chemisorption. [d] TOFs

for acetophenone (TOF_{Aph}), benzaldehyde (TOF_{BA}) and butyrophenone (TOF_{Bph}) over Pd catalysts were calculated at the conversion of about 10 % of reactant.

The effect of Pd loading on the support materials was investigated by XRD. Both silica and silica-alumina support were highly amorphous in nature. Only a very broad peak at $2\theta = 25^{o}$ corresponding to amorphous silica can be observed in XRD patterns (Figure 2).[14] The weak diffraction peaks at 42° and 48° were assigned to Pd (111) and Pd (200) on Pd nanocatalysts, respectively. Pd/Al_2O_3 catalysts exhibit similar diffraction patterns to the Al_2O_3 support reported in literature.[19] No obvious change of crystal structure can be observed among Pd particles with different size on the all supports. Since XRD is less sensitive to small particles such as Pd particles under current study, the dispersion of surface Pd atoms was obtained by CO chemisorption experiments and summarized in Table 1, which decreased with increasing the Pd particle size but independent from the support surface areas.

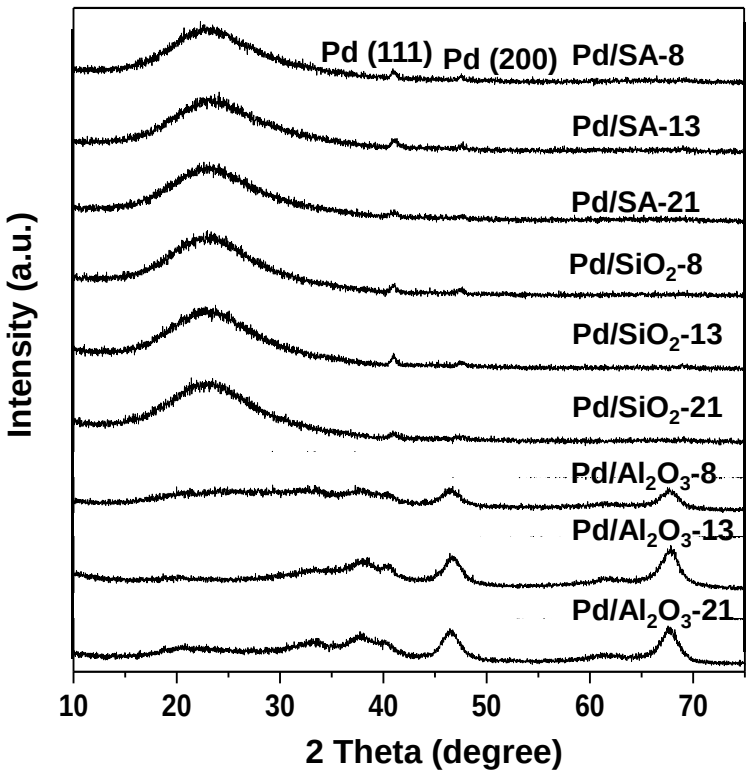

Figure 2. XRD patterns of different types of supported Pd-nanoparticle catalysts.

The effect of Pd particles on the local structure of support was investigate by ^{27}Al MAS NMR spectroscopy. As shown in Figure 3, a strong signal of octahedral coordinated Al (Al^{VI}) at -3 ppm and a weak signal of tetrahedral coordinated Al (Al^{IV}) at 51.8 ppm have been observed for all Pd/Al_2O_3 catalysts, typically for the ^{27}Al NMR spectra of γ-Al_2O_3.[3, 35] Compared to Pd/Al_2O_3 catalysts, the content of Al^{IV} (signal at 51.8 ppm) was significantly enhanced in Pd/SA catalysts. The ^{27}Al MAS NMR spectra of Pd/SA is similar to that reported for amorphous silica-alumina supports in literature.[33] Clearly, the ^{27}Al MAS NMR spectra of Pd/Al_2O_3 and Pd/SA catalysts demonstrated that the loading process and various Pd particle sizes cannot strongly influence the support structure and coordination. Often, Al^{VI} species in alumina and silica-alumina are associated to the formation of surface Lewis acid sites (LAS). The enhanced content of Al^{IV} in silica-alumina has been widely accepted to the incorporation of Al into the silica network, which can interact and enhance the acid strength of neighboring SiOH groups, acting as surface Brønsted acid sites.[33, 36, 37]

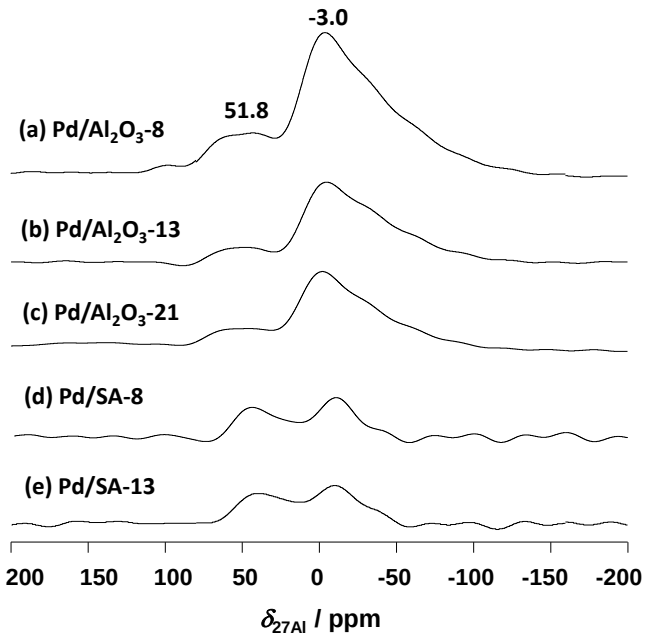

Figure 3. ^{27}Al MAS NMR spectra of Pd catalysts on alumina (a-c) and silica-alumina (d and e) supports.

Since the metal-support interaction induced by acidic support (e.g. alumina and silica-alumina) can strongly influence the catalytic performance of Pd catalysts,[3, 9, 19] the surface acidity of supported Pd catalysts are characterized by the temperature programmed desorption of ammonia (NH_3-TPD) experiments. As shown in Figure 4 and Figure S5, nearly no desorption peaks can be observed for Pd/SiO_2 catalysts since amorphous SiO_2 is a neutral support. Broad strong peaks were observed for both Pd/SA and Pd/Al_2O_3 catalysts with desorption maximum peak (*T*m) cantered at 240 ºC and 205 ºC, respectively, indicating a significant amount of acid sites generated on the supports. γ-Al_2O_3 was a typical Lewis acidic catalyst,[38] and thus, the peak at 205 ºC observed with Pd/Al_2O_3 catalysts has been assigned to ammonia adsorbed on LAS on alumina support. Alternatively, the peak at 240 ºC was assigned to BAS generated on silica-alumina, which is generated by introducing Al atoms into the silica network, and can only be formed on amorphous silica-alumina among these three supports. Often, the relative strength of the acid sites can be scaled by their *T*m, for instance the higher *T*m the higher acid strength. Therefore, the acid sites on Pd/SA showed acid sites seems stronger than those on Pd/Al_2O_3.

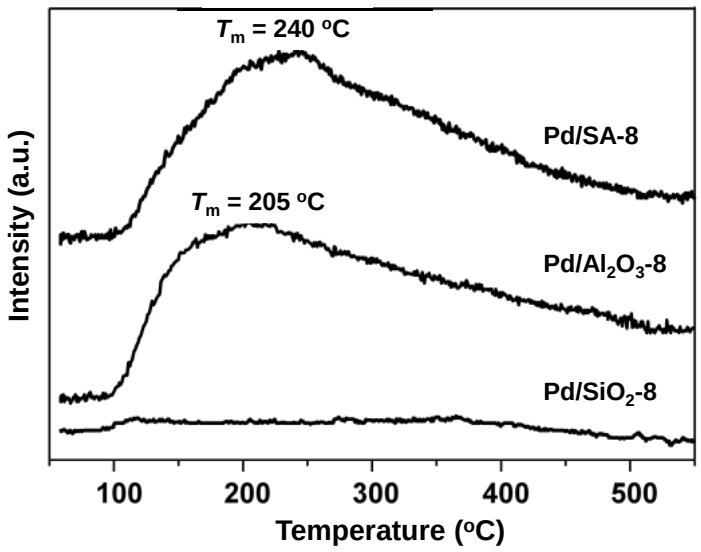

Figure 4. NH_3-TPD profiles of Pd catalysts with a particle size of 8 nm on various supports.

The interaction between acidic supports and metal nanocatalysts can introduce an ionic effect on active metal species.[15, 39] This effect can strongly influence the surface electronic properties of metal catalysts, which is crucial to the chemoselectivity of supported metal nanocatalysts in hydrogenation reactions.[1, 9, 14, 19] Often, the surface electronic properties of the Pd nanoparticles can be determined by XPS.[15, 19] As shown in Figure 5, the binding energy of Pd particles on different supports are all similarly, exhibiting two signals at 334.8 eV for Pd $3d_{5/2}$ and 340.2 eV for Pd $3d_{3/2}$. It indicates that the electronic properties of Pd particles are similar, independent from the support properties. Normally, surface acid sites can withdraw electrons from the metal particles via ionic effect. A higher acidity results in a higher binding energy.[15] Our recent work shows that the strength of acid sites is the key to tune the electronic properties of Pd particles on acidic support.[14] In this work, Pd particles exhibit similar electronic properties over support with different acidic properties as indicated by NH_3-TPD. The similar binding energy may indicate the metal-support interaction is very weak in supported Pd nanocatalysts prepared in this work, and consequently, the acid sites on support are hardly to withdraw electron density from metal

component. This is similar to that observed in Pd/SA prepared by double flame-spray pyrolysis technique.[19] In that work, the electron properties of Pd particles is almost the same over support materials with various strength and density of acid sites, which has been attributed to minimize the ionic effect through decoupling the formation of Pd particles and supports, one could efficiently from supports on Pd catalysts.

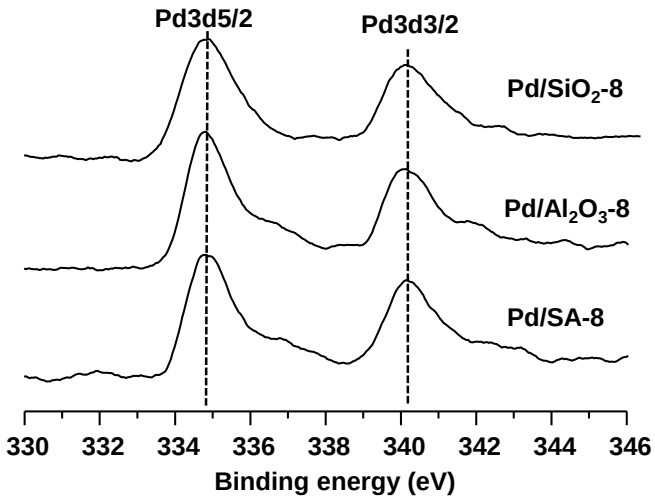

Figure 5. Binding energy of $Pd3d_{5/2}$ and $Pd3d_{3/2}$ lines of Pd catalysts with a particle size of 8 nm on various supports

Chemoselective hydrogenation. The performance of the obtained Pd catalysts was tested in the hydrogenation of acetonphenone (Aph), benzaldehyde (BA) and butyrophenone (Bph), and the proposed reaction pathway are described in Scheme S1. It is desired to the chemoselective hydrogenation to C=O bond to produce unsaturated alcohols, while those produced by hydrogenation of aromatics are the main byproducts. In hydrogenation reactions, the chemoselectivity is sensitive to the surface electronic properties of metal catalysts. Generally, the ionic effect induced by acidic supports leads to different surface electronic properties of metal catalysts, and thus, provide different chemoselectivity in hydrogenations. In the hydrogenation of

BA at 25 ºC under 3 bar hydrogen, mainly benzyl alcohol can be detected by GC analysis, which indicates all the catalysts exhibited an excellent chemoselectivity (100%) to the hydrogenation of the carbonyl group rather than aromatic rings in BA. This has been attributed to similar surface electronic properties of Pd nanoparticles, similar as observed in earlier studies.[14, 19] Moreover, it demonstrates that the various functional groups (neutral for Pd/SiO_2, Lewis acid sites for Pd/Al_2O_3 and Brønsted acid sites for Pd/SA catalyst) and different densities/strengths of acid sites on the supports, cannot significantly influence the chemoselectivity of Pd catalysts in hydrogenation reaction.

The conversion of BA as a function of time was shown in Figure 6 and corresponding TOFs at 10% conversion of BA are summarized in Table1. All catalysts are active in the conversion of BA. Reducing Pd particle size from 21 to 8 nm can significantly enhance the conversion of BA. For instance, Pd/SA-8 obtained ca. 100% conversion of BA after 3 h reaction, and only 65% and 50% for Pd/SA-13 and Pd/SA-21, respectively. A similar trend was observed for the TOFs of Pd/SA (5.2×10^{-2} s^{-1}, 4.5×10^{-2} s^{-1} and 3.2×10^{-2} s^{-1} for Pd/SA-8, Pd/SA-13, and Pd/SA-21, respectively). Pd/SiO_2 and Pd/Al_2O_3 showed similar tendencies as observed for Pd/SA, although they were characterized with different acidic properties. With respect to the same electronic properties of Pd catalysts and support properties as revealed by XPS and NH_3-TPD analysis, a size effect on the catalytic performance of Pd particles has been probed directly. In general, small particles can result in more defects (e.g. Pd atoms on the corner) than large particles, acting as active sites in catalytic reactions.[40] It has been reported that the low coordinated sites in the small particles due to the short-range ordering shows a significantly higher catalytic performance compared to those having larger particle size.[41] Moreover, smaller particle size can inhibit the hydrogen atoms diffuse deeply into the bulk with large particle size, and thus, hydrogen are readily available for the

reaction at the surface.[42] In addition, the product is easy to desorb due to the relatively lower enthalpy desorption on low-coordinated Pd sites, which may result in an increase in the conversion.[43] Therefore, the smaller Pd particle size and higher Pd dispersion are mainly response for the catalytic enhancement.

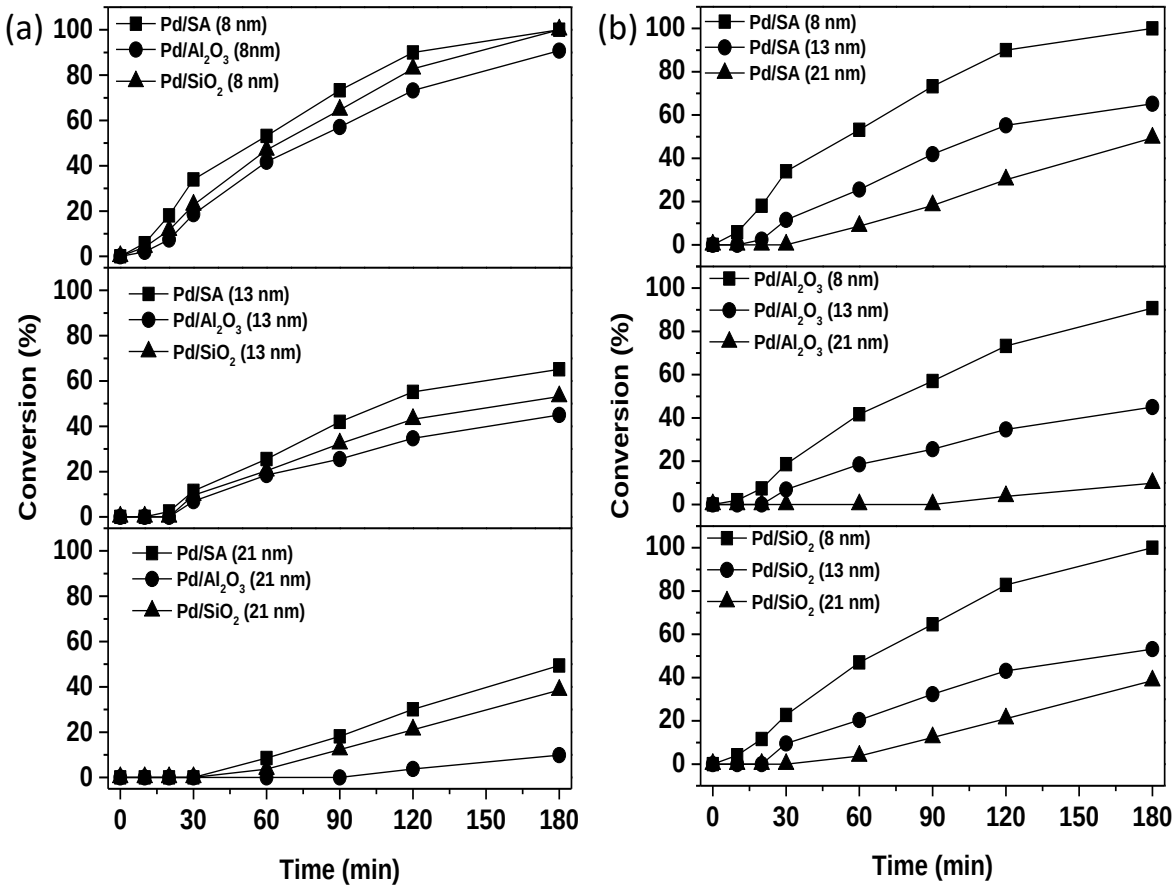

Figure 6. Conversion of benzoaldehyde (BA) over different supported Pd catalysts by (a) Pd particle sizes and by (b) supports (alumina-silica, SiO_2, and Al_2O_3 supports), as a function of reaction time at 3 bar of hydrogen and 25 ºC.

It should be noted that the TOFs should be similar with Pd particles having the same morphology (size, dispersion and lattice structure) and electronic properties. However, the TOFs are differ significantly for the same Pd particles on different supports in the BA hydrogenation. Silica-alumina supported catalysts exhibited better performance than the other two catalysts, e.g. 5.2 ×

10^{-2} s^{-1}, 4.2 × 10^{-2} s^{-1} and 3.2 × 10^{-2} s^{-1} for Pd/SA-8, Pd/SiO_2-8, and Pd/Al_2O_3-8, respectively. Although no obvious ionic effect on Pd particles can be induced by BAS on silica-alumina support, BAS can enhance the surface diffusion of BA on Pd/SA catalyst. This is similar as reported earlier that BAS can increase the concentration of BA in the local environment of Pd-sites, thereby increasing the accessibility of BA to Pd active sites.[19] LAS on the Al_2O_3 support can also adsorb BA on Pd/Al_2O_3 surface. However, LAS are often probed with the strong adsorption and activation of C=O over BAS.[36, 44] Compared to LAS, reactant adsorbed on the flexible SiOH sites on surface can easily interact with the metal nanocatalyst on the surface. With respect to the neutral silica support having larger surface area, it may improve the surface diffusion of BA on Pd/SiO_2 than on Pd/Al_2O_3, providing a higher TOFs.

Similar chemoselective hydrogenation results were obtained using acetophenone (Aph) and butyrophenone (Bph) as shown in Figure S6. A 100 % selectivity to C=O hydrogenation was obtained over all catalysts. The catalysts containing the small-size Pd particles (ca. 8 nm) all achieved a 100 % conversion of Aph and Bph after 8 hours reaction, while those having large-size Pd particles (ca. 21 nm) provide less than 50 % conversion under the same conditions. Both of Aph and Bph are less active than BA due to the strong electron density of carbonyl oxygen. In all reaction, the size effect is more significant than the effect of support acidity. This can be explained by Pd particle sizes are the active sites for hydrogen dissociation and hydrogenation reactions, while the support mainly governs the surface diffusion of reactants and products. Therefore, the understanding of the adsorption-desorption balance of each species involved and the behaviour of metal and supports is of great importance.

■ Conclusion

In this study, size-controlled Pd particles (8, 13, and 21 nm) were prepared by the colloidal method and then loaded on silica-alumina, Al_2O_3, and SiO_2 supports which have various acidities (BAS, LAS, and very weak SiOH, respectively) as observed in NH_3-TPD. Pd nanoparticles exhibit similar surface lattice structure and electronic properties as revealed by TEM, XRD and XPS analysis. Therefore, these catalysts are applied to investigate the effect of Pd particle size and the support acidity on their catalytic performance in the chemoselective hydrogenation of three chemicals (acetophenone, benzaldehyde, and butyrophenone) from bio-oil, combined with molecular dynamics study.

It has been found the chemoselectivity mainly relied on the Pd surface electronic properties. The particle size has a significant effect on the catalytic performance of these catalysts. Regardless of the type of the support (i.e., the type of acidity), catalysts with the smallest (8 nm) Pd particle size exhibit the highest conversion of the three model compounds compared to the catalysts of the medium (13 nm) and the largest (21 nm) Pd particle sizes. This has been explained by the smaller particle size provides more corner Pd atoms, higher surface hydrogen atom to reactant, and more low-coordinated sites.

Pd/SA catalysts (BSA containing on the support) showed the highest conversion and TOF compared to Pd/Al_2O_3 and Pd/SiO_2 catalysts. This might be due to the enhanced the diffusion rates of the chemicals on the surface of the catalysts although they could not induce the ionic effect from the metal surface. The reactants could be desorbed from support surface and diffused to the metal particle surface for hydrogenation. Interestingly, Pd/SiO_2 catalysts have both a slightly higher catalytic activity and TOFs than Pd/Al_2O_3 catalysts (LAS containing on the support). It could be due to the larger specific surface area on the silica support and the flexible SiOH groups on surface

that make the easy interaction possible with the metal particles on the surface. The results of this study indicate that the catalytic activities were influenced more by the particle size than the acidity of the support.

ASSOCIATED CONTENT

Supporting Information.

The following files are available free of charge.

TEM and HRTEM images, particle size distribution of supported Pd catalysts, NH_3-TPD profiles for supported Pd catalysts, calculated diffusivity of reactants and product on supported Pd catalysts, adsorption of acetophenone on various supports, conversion of butyrophenone over different Pd particle size on various supports.

AUTHOR INFORMATION

Corresponding Author

*jun.huang@sydney.edu.au (J. Huang). *Aibing.Yu@monash.edu.au (A.Yu).

Author Contributions

The manuscript was written through contributions of all authors. All authors have given approval to the final version of the manuscript.

ACKNOWLEDGMENT

J.H. K.K. and Z.W. acknowledge the financial supports from Australian Research Council Discovery Projects (DP150103842). J.H. acknowledges the Australian Research Council Discovery Projects (DP150103842 and DP180104010), the SOAR Fellowship, and the Sydney

Nano Grand Challenge from the University of Sydney for the support of this project. J.H. thanks Faculty's Energy & Materials Clusters and MCR scheme and the International Project Development Funding at the University of Sydney.

KEYWORDS: Chemoselective hydrogenation, Heterogeneous catalyst, Shape confined cubic Pd catalysts, Silica/alumina supports, Support acidity

REFERENCES

[1]. M. M. Chen, N. Maeda, A. Baiker and J. Huang, *ACS. Catal.*, **2012**, 2, 2007.

[2]. G. W. Huber, S. Iborra and A. Corma, *Chem. Rev.*, **2006**, 106, 4044.

[3]. K. D. Kim, S. Pokhrel, Z. C. Wang, H. J. Ling, C. F. Zhou, Z. W. Liu, M. Hunger, L. Madler and J. Huangt, *ACS. Catal.*, **2016**, 6, 2372.

[4]. C. Mohr, H. Hofmeister, J. Radnik and P. Claus, *J. Am. Chem. Soc.*, **2003**, 125, 1905.

[5]. A. Corma and P. Serna, *Science*, **2006**, 313, 332.

[6]. C. Mohr, H. Hofmeister and P. Claus, *J. Catal.*, **2003**, 213, 86.

[7]. H. J. Wei, C. Gomez, J. J. Liu, N. Guo, T. P. Wu, R. Lobo-Lapidus, C. L. Marshall, J. T. Miller and R. J. Meyer, *J. Catal.*, **2013**, 298, 18.

[8]. E. Ronzon and G. Del Angel, *J. Mol. Catal. A. Chem.*, **1999**, 148, 105.

[9]. J. Huang, Y. J. Jiang, N. van Vegten, M. Hunger and A. Baiker, *J. Catal.*, **2011**, 281, 352.

[10]. F. Hoxha, B. Schimmoeller, Z. Cakl, A. Urakawa, T. Mallat, S. E. Pratsinis and A. Baiker, *J. Catal.*, **2010**, 271, 115.

[11]. F. Jiang, L. Zeng, S. R. Li, G. Liu, S. P. Wang and J. L. Gong, *ACS Catal.*, **2015**, 5, 438.

[12]. Y. F. He, J. X. Fan, J. T. Feng, C. Y. Luo, P. F. Yang and D. Q. Li, *J. Catal.*, **2015**, 331, 118.

[13]. C. F. Xu, G. X. Chen, Y. Zhao, P. X. Liu, X. P. Duan, L. Gu, G. Fu, Y. Z. Yuan and N. F. Zheng, *Nat. Commun.*, **2018**, 9.

[14]. Z. C. Wang, K. D. Kim, C. F. Zhou, M. M. Chen, N. Maeda, Z. W. Liu, J. Shi, A. Baiker, M. Hunger and J. Huang, *Catal. Sci. Technol.*, **2015**, 5, 2788.

[15]. B. L. Mojet, J. T. Miller, D. E. Ramaker and D. C. Koningsberger, *J. Catal.*, **1999**, 186, 373.

[16]. F. K. Shieh, S. C. Wang, C. I. Yen, C. C. Wu, S. Dutta, L. Y. Chou, J. V. Morabito, P. Hu, M. H. Hsu, K. C. W. Wu and C. K. Tsung, *J. Am. Chem. Soc.*, **2015**, 137, 4276.

[17]. G. Darabdhara, P. K. Boruah, P. Borthakur, N. Hussain, M. R. Das, T. Ahamad, S. M. Alshehri, V. Malgras, K. C. W. Wu and Y. Yamauchi, *Nanoscale*, **2016**, 8, 8276.

[18]. K. Murata, Y. Mahara, J. Ohyama, Y. Yamamoto, S. Arai and A. Satsuma, *Angew. Chem. Int. Edit.*, **2017**, 56, 15993.

[19]. Z. C. Wang, S. Pokhrel, M. M. Chen, M. Hunger, L. Madler and J. Huang, *J. Catal.*, **2013**, 302, 10.

[20]. T. Kimura, T. Miyazawa, J. Nishikawa, S. Kado, K. Okumura, T. Miyao, S. Naito, K. Kunimori and K. Tomishige, *Appl. Catal. B. Environ.*, **2006**, 68, 160.

[21]. S. Handjani, E. Marceau, J. Blanchard, J. M. Krafft, M. Che, P. Maki-Arvela, N. Kumar, J. Warna and D. Y. Murzin, *J. Catal.*, **2011**, 282, 228.

[22]. H. W. Chen, C. S. Chen and S. J. Harn, *J. Phy. Chem.*, **1995**, 99, 10557.

[23]. F. Pinna, F. Menegazzo, M. Signoretto, P. Canton, G. Fagherazzi and N. Pernicone, *Appl. Catal. A. Gen.*, **2001**, 219, 195.

[24]. N. Perret, F. Cardenas-Lizana and M. A. Keane, *Catal. Commun.*, **2011**, 16, 159.

[25]. P. Gallezot and D. Richard, *Catal. Rev. Sci. Eng.,* **1998**, 40, 81.

[26]. Y. Yuan, Y. V. Kaneti, M. S. Liu, F. Z. Jin, D. F. Kennedy, X. C. Jiang, J. Huang and A. B. Yu, *J. Energy. Chem.*, **2015**, 24, 660.

[27]. Y. Li, E. Boone and M. A. El-Sayed, *Langmuir*, **2002**, 18, 4921.

[28]. Y. E. Wu, S. F. Cai, D. S. Wang, W. He and Y. D. Li, *J. Am. Chem. Soc.*, **2012**, 134, 8975.

[29]. J. B. Wu, A. Gross and H. Yang, *Nano Lett.*, **2011**, 11, 798.

[30]. V. Tohver, J. E. Smay, A. Braem, P. V. Braun and J. A. Lewis, *P. Natl. Acad. Sci.*, **2001**, 98, 8950.

[31]. M. S. Jin, H. Y. Liu, H. Zhang, Z. X. Xie, J. Y. Liu and Y. N. Xia, *Nano. Res.*, **2011**, 4, 83.

[32]. T. H. Yang, S. Zhou, K. D. Gilroy, L. Figueroa-Cosme, Y. H. Lee, J. M. Wu and Y. N. Xia, *P. Natl. Acad. Sci.*, **2017**, 114, 13619.

[33]. E. J. M. Hensen, D. G. Poduval, P. C. M. M. Magusin, A. E. Coumans and J. A. R. van Veen, *J. Catal.*, **2010**, 269, 201.

[34]. D. M. Ladd, A. Volosin and D. K. Seo, *J. Mater. Chem.*, **2010**, 20, 5923.

[35]. R. Feng, S. T. Liu, P. Bai, K. Qao, Y. H. Wang, H. A. Al-Megren, M. J. Rood and Z. F. Yan, *J. Phys. Chem. C.*, **2014**, 118, 6226.

[36]. J. Huang, N. van Vegten, Y. J. Jiang, M. Hunger and A. Baiker, *Angew. Chem. Int. Edit.*, **2010**, 49, 7776.

[37]. Z. C. Wang, Y. J. Jiang, O. Lafon, J. Trebosc, K. D. Kim, C. Stampfl, A. Baiker, J. P. Amoureux and J. Huang, *Nat. Commun.*, **2016**, 7.

[38]. G. Busca, *Chem. Rev.*, **2007**, 107, 5366.

[39]. A. Y. Stakheev, Y. Zhang, A. V. Ivanov, G. N. Baeva, D. E. Ramaker and D. C. Koningsberger, *J. Phys. Chem. C.*, **2007**, 111, 3938.

[40]. S. W. Cao, F. Tao, Y. Tang, Y. T. Li and J. G. Yu, *Chem. Soc. Rev.*, **2016**, 45, 4747.

[41]. R. Hess, F. Krumeich, T. Mallat and A. Baiker, *Catal. Lett.*, **2004**, 92, 141.

[42]. A. Binder, M. Seipenbusch, M. Muhler and G. Kasper, *J. Catal.*, **2009**, 268, 150.

[43]. W. Ludwig, A. Savara, R. J. Madix, S. Schauermann and H. J. Freund, *J. Phys. Chem. C.*, **2012**, 116, 3539.

[44]. Z. C. Wang, Y. J. Jiang, M. Hunger, A. Baiker and J. Huang, *ChemCatchem*, **2014**, 6, 2970.